

# Switched-Mode High-Efficiency Microwave Power Amplifiers In A Free-Space Power Combiner Array

Thomas B. Mader, Eric W. Bryerton, Milica Marković, Michael Forman, and Zoya Popović

*Abstract*— A design-oriented analysis of the microwave transmission-line class-E amplifier is presented. Experiments and harmonic-balance circuit simulations verify the theoretical equations which predict class-E amplifier output power, maximum frequency of operation, and DC-RF conversion efficiency. Experimental results at 0.5, 1, 2, and 5 GHz are presented. At 0.5 GHz, 83% drain efficiency and 80% power-added efficiency are measured with an output power of 0.55 W using the Siemens CLY5 MESFET. These results are compared to a class-A and class-F power amplifier using the same device. At 5 GHz, 81% drain efficiency and 72% power-added efficiency are measured with an output power of 0.61 W using the Fujitsu FLK052WG MESFET. Finally, the 5-GHz class-E power amplifier is successfully integrated into an active-antenna array, demonstrating power combining of four elements with an 85% power-combining efficiency. At 5.05 GHz, the class-E power amplifier antenna array delivers a total of 2.4 W of output power, with a DC-RF conversion efficiency of 74% and a power-added efficiency of 64%.

## I. INTRODUCTION

ACHIEVING high efficiency in microwave amplifiers is important for reducing the size and weight, and increasing the output power, battery lifetime, and reliability of portable wireless transmitters. By increasing the efficiency of an amplifier from 50% to 90%, the dissipated heat power is reduced by a factor of nine for the same output power. Currently, microwave amplifiers have demonstrated 72% power-added efficiency (PAE) with 1 W of output power at 12 GHz [1], 47% PAE with 0.5 W of output power at 20 GHz [2], and 29% PAE with 1 W of output power at 40 GHz [3]. Device technology is improving at a rapid pace; the intent of this work is to build upon these device improvements, enabling design and analysis of very high efficiency switched-mode power amplifiers.

The idea of harmonically tuning RF power amplifiers has existed since at least 1958 [4] and 1967 [5]. In both of these works, a short circuit is presented to the output of the transistor (or vacuum tube) at even harmonics, and an open circuit is presented at all of the odd harmonic frequencies. In [6], Raab coins the term “class F” for this type of harmonically tuned amplifier operation. Since the 1980s numerous researchers have successfully applied the class-F concept to microwave solid-state power amplifiers [7]–[9].

The class-E amplifier, invented in 1975 by the Sokals [10], is particularly promising for high-frequency high-efficiency power generation. In [11], Raab first makes the assumption

T. Mader and M. Marković were with the University of Colorado. T. Mader is now with Hughes Aircraft Space and Communications Group. M. Marković is now with Clarkson University. E. Bryerton, M. Forman, and Z. Popović are with the Department of Electrical and Computer Engineering, University of Colorado, Boulder, CO.

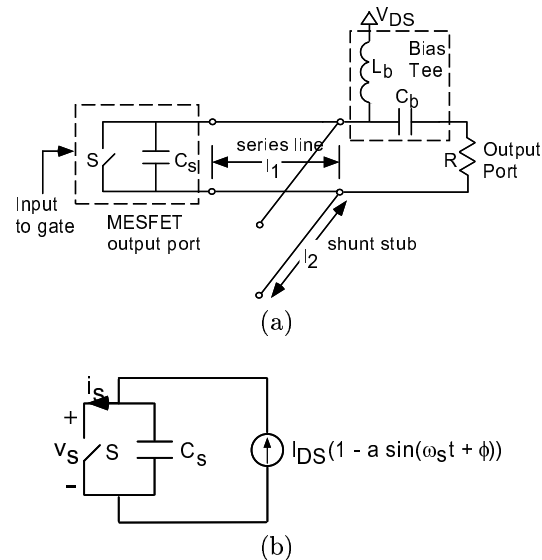


Fig. 1. (a) The transmission-line class-E high-efficiency circuit. (b) The class-E circuit assuming sinusoidal load current.

of sinusoidal current flow in the output of the class-E circuit used in this paper. Fig. 1(a) shows the class-E switched-mode amplifier topology. The active device, in this case a MESFET, acts as a switch, and the circuit must be properly designed to give class-E operation. At low RF frequencies, such circuits have demonstrated efficiencies as high as 96% [10]. At microwave frequencies, however, transistors are not ideal switches due to parasitic device capacitances. These parasitics can be deembedded from the device and included in the tuned circuit design [12]. The capacitance  $C_s$  in the circuit in Fig. 1(a) is the intrinsic output capacitance of the transistor, while the lead inductance of the device may be accounted for by shortening the series transmission line  $l_1$ . The efficiency is limited primarily by the drain-to-source saturation resistance of the transistor and the lossy properties of its parasitic elements. It is shown here that even in a degraded class-E mode, high efficiency and power can still be achieved.

Recently the transmission-line class-E amplifier has been experimentally demonstrated at 0.5, 1, and 2 GHz [12]. In this paper, a design-oriented analysis of the transmission-line class-E amplifier is presented and experimental results are extended to 5 GHz. Harmonic-balance circuit simulations verify that the amplifiers operate in class-E mode. Finally, the 5-GHz class-E transmission-line amplifier is integrated into an active-antenna power-combining array.

## II. DESIGN-ORIENTED ANALYSIS OF CLASS-E AMPLIFIERS

### A. Assumptions Made In The Analysis

There are several assumptions made in the simplified analysis of the class-E circuit presented here (see Fig. 1(a)).

- A 50% duty cycle is used. This is shown in [11] to be the optimal case.
- The switching device has zero on-resistance and infinite off-resistance.
- The shunt capacitor  $C_s$  is the output capacitance of the transistor and is assumed to be linear in the initial analysis.
- $L_b$  acts as an ideal bias choke (open circuit at RF).
- There are no losses in the circuit shown in Fig. 1(a), except into the load R. Therefore, all of the DC power,  $V_{DS}I_{DS}$ , is dissipated in R (100% efficiency operation).
- The external load network has a high  $Q$ -factor and constrains the current flowing into it to be approximately sinusoidal at the switching frequency.

These assumptions simplify the basic explanation of the class-E circuit significantly and allow tractable equations to describe its operation [11]. The exact time domain solution of the class-E switched-mode circuit involves a set of differential equations which give little insight into the basic tradeoffs of the circuit, are tedious to solve, and are not useful for design [13].

### B. Switch Voltage and Current Waveforms

The assumptions used in this analysis are illustrated in Fig. 1(b). An equivalent current source, which consists of a constant (DC) and sinusoidal (RF) component, is placed across the switched capacitor. The class-E amplifier is thus reduced to a simple first-order circuit.

It is seen in Fig. 1(b), when the switch is turned ON, there is no voltage across the switch, but a piece of sinusoidal current (with a DC component) flows through it. When the switch turns OFF, the sinusoidal current continues to flow, but now it flows through the shunt capacitive part of the switch. During the OFF interval,

$$v_s(t) = \frac{1}{C_s} \int_0^t I_{DS}(1 - a \sin(\omega_s t' + \phi)) dt'. \quad (1)$$

The integral implicitly assumes that  $v_s(0) = 0$ , which is one of the three boundary conditions imposed upon  $v_s(t)$  by definition of class E. Thus

$$v_s(t) = \frac{I_{DS}}{\omega_s C_s} (\omega_s t + a(\cos(\omega_s t + \phi) - \cos \phi)). \quad (2)$$

The other two conditions for class-E operation are  $v_s(\frac{T_s}{2}) = 0$  and  $\frac{dv_s}{dt}(\frac{T_s}{2}) = 0$ . The first condition avoids shorting the capacitor  $C_s$  when there is voltage across it during switching, and the second condition ensures a "soft" turn-on condition for the switching device. These two additional constraints determine  $a$  and  $\phi$  uniquely:

$$a = \sqrt{1 + \frac{\pi^2}{4}} \simeq 1.862, \quad (3)$$

$$\phi = -\arctan \frac{2}{\pi} \simeq -32.48^\circ. \quad (4)$$

$a$  and  $\phi$  are constants for *any* high- $Q$  class-E circuit with a capacitor in shunt with the switch and a 50% duty cycle. Now the voltage and current across the switch are known and are plotted in Fig. 2.

### C. Relationship Between $V_{DS}$ and $I_{DS}$

It is of interest to find the relationship between  $V_{DS}$  and  $I_{DS}$ , or in other words, how much current is drawn for a given supply voltage or vice-versa.  $V_{DS}$  is the DC component of  $v_s(t)$ , the voltage across the switch. Taking the time average of the switch voltage over the period gives  $V_{DS} = \frac{I_{DS}}{\pi \omega_s C_s}$ , so that the DC power is given by:

$$P_{DC} = I_{DS}V_{DS} = \pi \omega_s C_s V_{DS}^2 \quad (5)$$

This simple result has important implications for a practical microwave class-E circuit, assuming that the minimum value of  $C_s$  is the parasitic capacitance of a microwave device, for example  $C_{ds}$  of a MESFET. At a specified frequency, a device with an output capacitance  $C_s$  must operate at some supply voltage  $V_{DS}$ . Since  $\omega_s$ ,  $C_s$ , and  $V_{DS}$  are now specified, the device must be able handle the required maximum current, which is  $(1 + a)I_{DS} \simeq 2.86I_{DS}$ . Due to this transistor limitation, an approximate maximum frequency of class-E operation can be found for a given device:

$$f_{max} = \frac{I_{DS}}{2\pi^2 C_s V_{DS}} = \frac{I_{max}}{C_s V_{DS}} \frac{1}{2\pi^2(1+a)} \simeq \frac{I_{max}}{56.5 C_s V_{DS}}. \quad (6)$$

For higher drain bias voltages, the maximum frequency of operation decreases. For example, the Siemens CLY5 MESFET considered in the next section has  $I_{max} \simeq 1200$  mA and  $C_s \simeq 2.6$  pF. For this transistor at a DC drain voltage of  $V_{DS} = 6$  V,  $f_{max} \simeq 1.4$  GHz. Above these frequencies, this device cannot be used for an *ideal* class-E circuit, although an approximation to class-E operation may be obtained at higher frequencies with some degradation in maximum achievable efficiency [14].

### D. Fundamental-Frequency Class-E Load Impedance

Finding the DC component of  $v_s(t)$  yields an expression relating the DC parameters of the class-E circuit ( $V_{DS}$  and  $I_{DS}$ ). Finding the fundamental-frequency component of  $v_s(t)$  yields information about the RF impedances in the circuit. The fundamental component of current flowing into the load network,  $i_{net1}$ , was found above (its magnitude is  $aI_{DS}$  and its phase is  $\phi$ ). However, the fundamental component of the load voltage,  $v_{s1}$ , must be found using Fourier-series expansions. Only the results are presented here:

$$v_{s1} = a_0 I_{DS} \sin(\omega_s t + \phi_0) \quad (7)$$

$$i_{net1} = a I_{DS} \sin(\omega_s t + \phi), \quad (8)$$

where the constants  $a_0$  and  $\phi_0$  are given by:

$$a_0 = \frac{1}{\omega_s C_s} \sqrt{\frac{\pi^2}{16} + \frac{4}{\pi^2} - \frac{3}{4}}, \quad (9)$$

$$\phi_0 = \frac{\pi}{2} + \arctan\left(\frac{2\pi}{8 - \pi^2}\right). \quad (10)$$

and  $a$  and  $\phi$  are given in (3) and (4). The phasor impedance of the external load network can now be found:

$$Z_{net1} = \frac{a_0}{a} e^{j(\phi_0 - \phi)} = \frac{\kappa_0}{\omega_s C_s} e^{j\theta_0} \simeq \frac{0.28015}{\omega_s C_s} e^{j49.0524^\circ}. \quad (11)$$

The required load angle for class-E operation with a capacitor in shunt with the switch is a constant. To ensure class-E operation, all that is needed is a specific fundamental impedance of  $Z_{net1}$ , and open-circuit conditions at all of the higher harmonic frequencies. Applying standard transmission-line formulas to the transmission-line load network topology shown in Fig. 1(a), two equations are found relating the transmission line lengths and characteristic admittances to produce the desired fundamental impedance condition [12]. The electrical lengths of lines  $l_1$  and  $l_2$  should be close to  $45^\circ$ , so that an approximate open circuit will be presented to the switched capacitor at the second harmonic. The characteristic impedances of the lines may be adjusted to enforce this condition. Additional methods of enforcing harmonic open circuit conditions are described in [13]. For a packaged device, the lead inductance connecting the switched capacitor to the series transmission line  $l_1$  is significant; this is accounted for by shortening the length of  $l_1$ .

### E. Fourier Series of Switch Voltage

The simplified analysis of the class-E circuit given above assumes a sinusoidal output signal at the load resistor  $R$ . In practice, some residual higher-harmonic components will be present at the output of the circuit, depending upon the particular choice of load network topology and specific design values for the elements. In this section, the switch voltage  $v_s(t)$  found above is analyzed using Fourier series, and expressions for the magnitude and phase of the harmonics of switch voltage are given. These general results can then be transformed through any specific load network to find explicit expressions for the harmonic content at the output of the class-E amplifier. Furthermore, it is shown that a good approximation to class-E operation may be obtained with only two harmonics of the switch voltage waveform.

An expression for switch voltage  $v_s(t)$  was derived in Eqs. 2–4. The Fourier series is defined as:

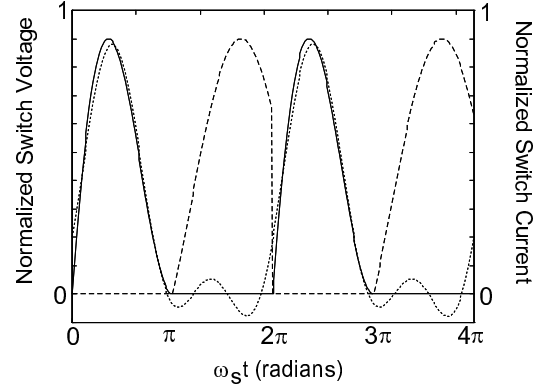


Fig. 2. The switch-voltage waveform with two harmonics taken into account (dotted line), plotted along with the ideal class-E switch-voltage waveform (solid line) and ideal current waveform (dashed line).

$$v_s(t) = \sum_{n=-\infty}^{\infty} K_n e^{jn\omega_s t}, \quad (12)$$

$$K_n = \frac{I_{DS}}{2\pi\omega_s C_s} \int_0^{\pi} ((\omega_s t) + a(\cos((\omega_s t) + \phi) - \cos \phi)) e^{-jn(\omega_s t)} d(\omega_s t). \quad (13)$$

The integration is performed only over the first half of the period, when  $v_s(t)$  is nonzero, and  $(\omega_s t)$  is used as the integration variable. The results are:

$$v_{sn}(t) = a_n I_{DS} \sin(n\omega_s t + \phi_n), \quad (14)$$

$$a_n = \frac{2|K_n|}{I_{DS}}, \quad \phi_n = \frac{\pi}{2} + \angle K_n, \quad (15)$$

$$(n \text{ odd}, n \neq 1): \quad K_n = \frac{I_{DS}}{\pi\omega_s C_s} \left(-\frac{1}{n^2}\right), \quad (16)$$

$$(n \text{ even}, n \neq 0): \quad K_n = \frac{I_{DS}}{\pi\omega_s C_s} \left(\frac{2n + j\pi}{2n(1 - n^2)}\right), \quad (17)$$

$$(n = 1): \quad K_1 = \frac{I_{DS}}{\pi\omega_s C_s} \left(\frac{\pi^2}{8} - 1 - \frac{j\pi}{4}\right). \quad (18)$$

These expressions may be used to find the magnitude and phase of any number of harmonics of the ideal class-E switch-voltage waveform. In Fig. 2, for example, the first two harmonics of the switch-voltage waveform are plotted along with the ideal waveforms. Only two harmonics of switch voltage show the salient form of class-E operation.

### F. Efficiency Analysis

For microwave class-E amplifiers using low-loss reactive elements (such as microstrip transmission lines), the majority of loss occurs within the transistor. During the OFF-state, the transistor looks primarily reactive (the intrinsic device looks like a capacitor at its output port), and during the ON-state, the transistor looks like a small resistor. It is the ON-state resistance, which may be estimated from the MESFET's I-V curves, which is primarily responsible for its lossy behavior. The transistor output port model used here is modified from the model proposed in [15].

As before, a sinusoidal load current is assumed. Analysis of the lossy circuit gives an expression for DC to RF conversion efficiency, or drain efficiency, ( $\eta_d$ ), in the case of a FET:

$$\eta_d = \frac{1 + (\frac{\pi}{2} + \omega_s C_s R_s)^2}{(1 + \frac{\pi^2}{4})(1 + \pi\omega_s C_s R_s)^2}. \quad (19)$$

This expression for drain efficiency shows that the product  $\omega_s C_s R_s$  is much less than unity for a practical high-efficiency class-E circuit. Initial assumptions dictate that this expression should only be used for drain efficiencies above 60%.

## III. EXPERIMENTAL RESULTS

### A. Comparison With Class A and Class F

In [12], three experimental class-E circuits are presented using the Siemens CLY5 MESFET at 0.5, 1, and 2 GHz. To compare the class-E amplifier with other topologies, a class-A and a switched-mode class-F amplifier are designed and built at 500 MHz using the same transistor and substrate as the class-E amplifier. The class-A and class-F amplifiers are designed using the values for  $C_s$  and  $L_s$  obtained when designing the class-E amplifier. The class-F amplifier is designed to present a short to the switch at the second harmonic. The fundamental is matched for maximum power delivered to the load.

The output power and power-added efficiency are measured as a function of input power level and frequency for both the class-A and class-F amplifiers and plotted together with the results for the 500-MHz class-E amplifier. The power sweep is plotted in Fig. 3, and the frequency sweep is plotted in Fig. 4. As the device is driven into saturation, the class-A amplifier is no longer class-A but class-AB. It is interesting to note that the gain of the class-E amplifier compresses at a lower input power level than the gain of the class F. This is because the second harmonic short in the class F flattens the switch voltage waveform, reducing the peak stresses on the transistor.

While the class-E amplifier yields the highest efficiency, Fig. 5 shows that for a given efficiency, the class-F amplifier generates more output power.

### B. Two Microstrip 5-GHz Class-E Power Amplifiers

For a higher frequency class-E power amplifier, two packaged MESFETs are considered, the Fujitsu FLK052WG

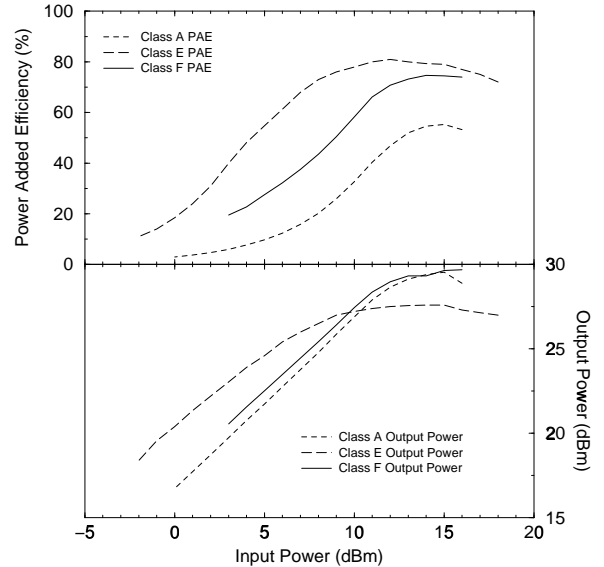


Fig. 3. Output power and power-added efficiency power sweeps for the 500-MHz Siemens CLY5 class-A ( $V_{DS}=5$  V,  $I_{DS}=318$  mA), class-E ( $V_{DS}=6$  V,  $I_{DS}=111$  mA), and class-F ( $V_{DS}=6$  V,  $I_{DS}=196$  mA) amplifiers.

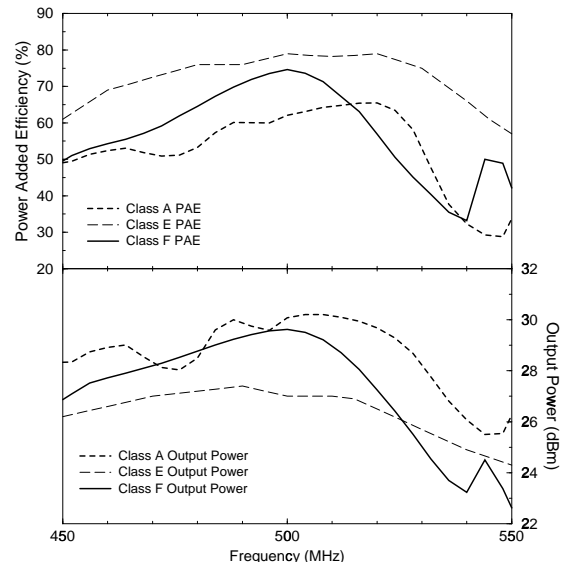


Fig. 4. Output power and power-added efficiency frequency sweeps for the 500-MHz Siemens CLY5 class-A, class-E, and class-F amplifiers.

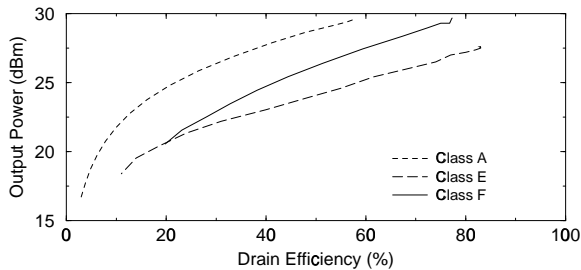


Fig. 5. Output power as a function of drain efficiency for the 500-MHz Siemens CLY5 class-A, class-E, and class-F amplifiers.

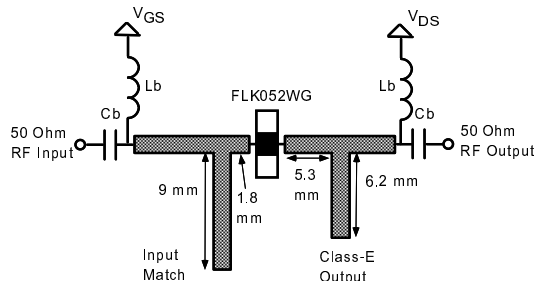


Fig. 6. The FLK052WG class-E microstrip power amplifier. This amplifier delivers 0.61 W into 50  $\Omega$ , with a compressed gain of 9.8 dB, a drain efficiency of 81%, and a power-added efficiency of 72% at 5.0 GHz. The substrate is Duroid with  $\epsilon_r = 2.2$ ,  $h = 0.508$  mm, and all lines are 50  $\Omega$  (1.6 mm wide).

and the FLK202MH-14. Both of these devices are designed for Ku-Band (12-15 GHz) power amplification. At these frequencies, these MESFETs operate at approximately 30% power-added efficiency. Using these devices at a lower frequency, such as 5 GHz, allows for the harmonic waveshaping required for class-E operation, analogous to using the 2.5 GHz CLY5 at 0.5 and 1 GHz.

For an initial design of the two class-E amplifiers, the output capacitance and inductance,  $C_s$  and  $L_s$ , of the devices are estimated using  $S$ -parameters given in the data sheets and knowledge of the expected approximate output power of the amplifiers at 5 GHz. The output power of the class-E amplifier is proportional to the capacitance across the switch in the circuit ( $C_s$ ). Eq. 11 is then used to design the output matching circuit.  $S$ -parameters are also used to design a single-stub input matching circuit for the two devices. These dimensions are used as a starting point for the experimental circuits, then the dimensions are experimentally adjusted until maximum power-added efficiency is obtained. The bias point and input power levels are also experimentally adjusted. The topology of these two class-E amplifiers is the same as the topology used for the amplifiers in [12], as shown in Fig. 6.

The FLK052WG class-E amplifier demonstrates an output power of 0.61 W, a compressed gain of 9.8 dB, a drain efficiency of 81%, and a power-added efficiency of 72% at 5 GHz. The input power is 18 dBm (63 mW). The FLK202MH-14 class-E amplifier demonstrates an output

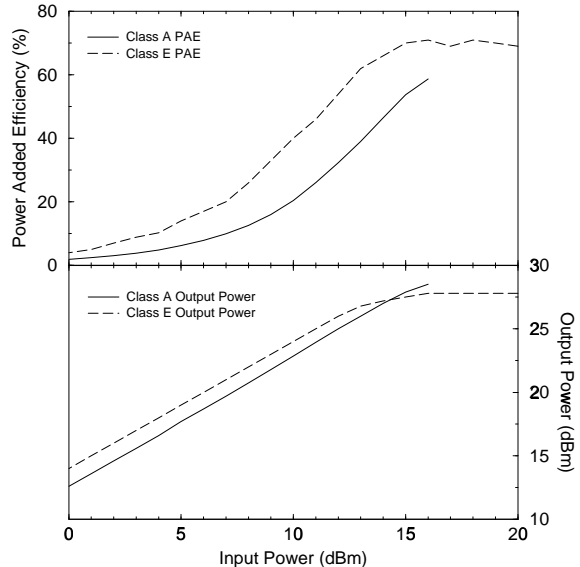


Fig. 7. Power sweep for the FLK052WG class-A ( $V_{DS}=8$  V,  $I_{DS}=128$  mA) and class-E ( $V_{DS}=8$  V,  $I_{DS}=93$  mA) amplifiers. Output power and power-added efficiency are plotted as a function of input power level.

power of 1.8 W, a compressed gain of 7.6 dB, a drain efficiency of 73%, and a power-added efficiency of 60% at 5.1 GHz. The input power is 25 dBm (316 mW). Although the FLK202MH-14 amplifier delivers a higher output power into 50  $\Omega$ , it operates at a lower efficiency, and it requires five times as much input power to operate in class-E mode.

The output power and power-added efficiency are measured as a function of input power level and frequency for the FLK052WG class-E amplifier. The results are plotted together with a class-A power amplifier using the same device. The power sweep is plotted in Fig. 7, and the frequency sweep is plotted in Fig. 8. The power-added efficiency is greater than 70% over a 5% bandwidth and greater than 60% over a 10% bandwidth.

#### IV. HARMONIC-BALANCE CIRCUIT SIMULATIONS

In order to verify that the fabricated circuits operate in class-E mode, five-tone harmonic-balance analysis is used to simulate the circuits with Compact Software's Harmonica [16]. A Materka-Kacprzak model [17] for the Siemens CLY5 MESFET supplied by Compact Software is used for the simulations.

Experimentally obtained amplifier circuits at 0.5 GHz, 1 GHz, and 2 GHz are simulated and the results are presented in Table I. Simulated current and voltage waveforms of the transistor have the characteristic shape of the ideal class-E circuit, as shown in Fig. 9. The discrepancies in efficiency and power simulations are larger for higher levels of saturation. We feel that the nonlinear models need to be improved for heavily saturated transistors. A good nonlinear model is unfortunately not available for the FLK052 MESFET, so no simulations are presented for amplifiers

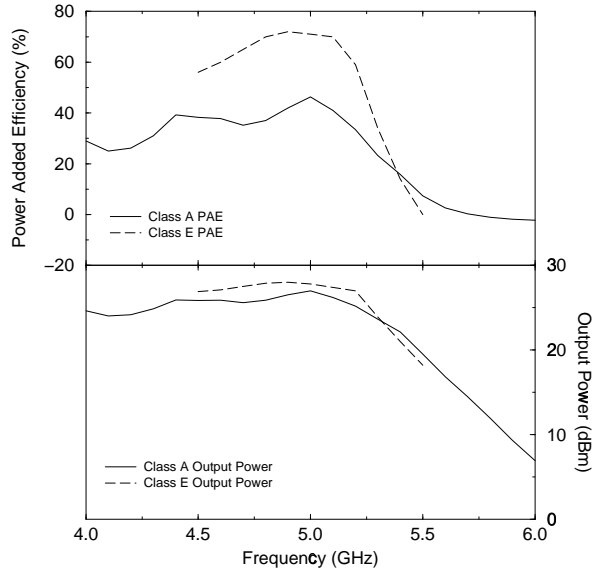


Fig. 8. Frequency sweep for the FLK052WG class-A and class-E amplifiers. Output power and power-added efficiency are plotted as a function of frequency of operation.

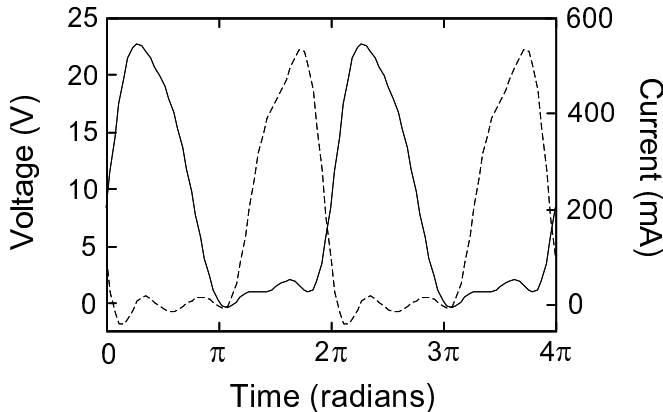


Fig. 9. Simulated voltage (solid line) and current (dashed line) waveforms at 500 MHz using the Materka model for the Siemens CLY5 MESFET.

using this device.

## V. A FREE-SPACE CLASS-E AMPLIFIER ARRAY

In this section, a high-efficiency active-antenna array, which amplifies a plane wave in transmission, is presented. Such arrays can be used for large-scale power combining [18]. In the active array presented here, a plane wave is incident on an array of antennas, each one connected to an amplifier input. The outputs of the amplifiers are each connected to an output antenna. The array of output antennas radiates an amplified plane wave [19]. If all of the amplifiers are in phase, their output powers are added in free space. It is also possible to focus the wave at the input and/or output in a lens amplifier, such as the one

f	PAE <sub>S</sub>	PAE <sub>M</sub>	Power <sub>S</sub>	Power <sub>M</sub>
0.5GHz	78.49%	80%	27.8dBm	27.4dBm
1GHz	72.49%	73%	30dBm	29.73dBm
2GHz	51.37%	54%	29.13dBm	27.24dBm

TABLE I

SIMULATED AND MEASURED VALUES FOR POWER-ADDED EFFICIENCY (PAE) AND OUTPUT POWER. A MATERKA-KACPRZAK NONLINEAR TRANSISTOR MODEL IS USED IN THE SIMULATIONS.

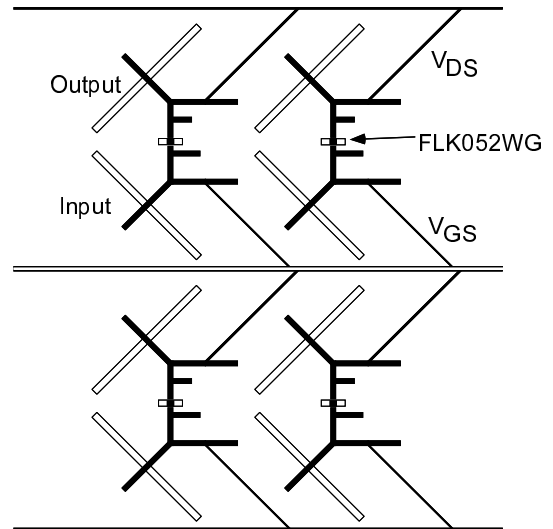


Fig. 10. The class-E power amplifier antenna array. This 4-element power-combining structure demonstrates 2.4 W of output power at 5.05 GHz, with 8.8 dB compressed gain, 74% drain efficiency, and 64% power-added efficiency. Antiresonant 50- $\Omega$  orthogonally polarized slot antennas couple the power between the amplifier and free-space, and half-wave microstrip lines provide bias to the Fujitsu FLK052WGs' gate and drain terminals.

demonstrated in [19]. Since the active elements are integrated within each input/output antenna pair, there is no feed circuitry. This reduces the size, complexity, loss and dispersion as compared to standard antenna arrays. In these two-dimensional power combiners, all of the dissipated power needs to be removed at the edges of the array, which could present inadequate heat sinking, especially around the center of the array. Therefore, efficiency is a prime concern, and it is addressed by integrating appropriate antenna elements with the class-E amplifiers described in section III. A 4-element active-antenna array is shown in Fig. 10. The amplifier circuits are microstrip, and the antennas are antiresonant slot antennas in the microstrip ground plane coupled to the microstrip feed lines.

### A. The Antiresonant Slot Antenna and Bias Network

An antiresonant slot antenna is chosen as the array radiating element. This type of antenna is broadband and can be designed to have a 50- $\Omega$  input impedance, as shown in [19]. Each of the antennas in the array are fed by an open microstrip line which extends about a quarter of a guided

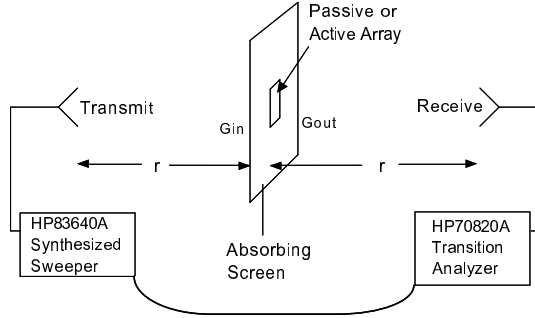


Fig. 11. Measurement setup for the 5 GHz class-E power amplifier array. First a passive structure is placed into the system (with  $50\text{-}\Omega$  lines connecting the input and output antennas), and a calibration power level is measured. Then the amplifier array is placed in the system, and the gain and power levels are determined.

wavelength ( $\lambda_g/4$ ) beyond the center of the slot. The open circuit is transformed to a short at the plane of the slot. A single antenna is measured to have a 2:1 VSWR bandwidth of 20% with a cross-polarization ratio of 23 dB at a center frequency of 5 GHz.

### B. High-Efficiency Amplifier Array Design and Measurements

In an active-antenna array, it is important to provide bias lines which do not affect the stability of the amplifier. As shown in Fig. 10, high-impedance bias lines are connected to the voltage nulls along the gate and drain circuit stubs. The amplifiers are the same as the Class-E amplifiers described in III. Both the input and output loads are now the antennas, which are frequency-dependent impedances equal to  $50\text{-}\Omega$  only at the fundamental 5-GHz frequency. The impedance of the slot antennas is unimportant at the second harmonic, since the open-circuit condition satisfied by the class-E circuit is not load-dependent. The input and output slot arrays are orthogonally polarized to provide input/output isolation and stability.

The free-space measurement setup is shown in Fig. 11. An absorbing aperture is placed halfway between two horn antennas and in the far field of both antennas. The Friis transmission formula can be applied to this setup two times from one horn to the other, and the amplifier gain can be calculated if the input and output passive antenna array gains are known [19]. For calibration, a passive array similar to the one from Fig. 10, but with  $50\text{-}\Omega$  through-lines instead of the amplifiers, is placed in the absorbing aperture. This calibration allows us to calculate the effect of the antennas on the power received at the second horn relative to the power transmitted from the first horn. When the amplifier is placed in the aperture, 10 W of power is required at the transmitter to saturate the amplifier with about 320 mW incident on the array in the far field. The array radiates a maximum of 2.4 W at 5.05 GHz with 74% drain efficiency, 64% PAE, and a compressed gain of 8.8 dB contributed by the transistors.

It is interesting to examine the power-combining effi-

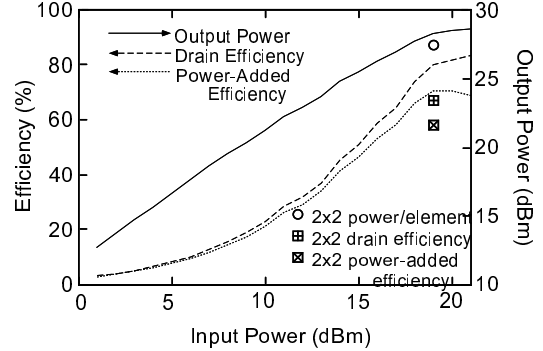


Fig. 12. Power sweep for the single cell class-E power amplifier element. Output power, drain efficiency, and power-added efficiency are plotted as a function of input power level. The results of the 2x2 amplifier array are superimposed on the graph; the output power in this case is plotted *per element*.

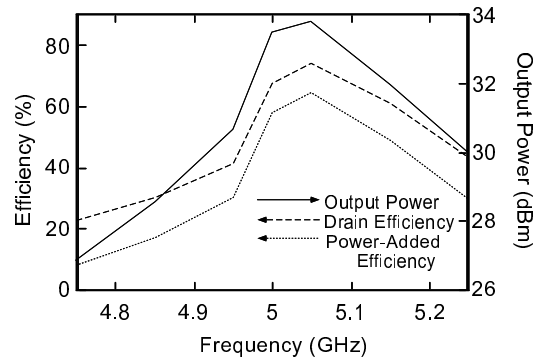


Fig. 13. Frequency sweep for the 2x2 class-E power amplifier array. Output power, drain efficiency, and power-added efficiency are plotted as a function of operating frequency. The input power level is +25 dBm at 5 GHz.

ciency of the array. At the design frequency of 5 GHz, a single element of the array radiates 0.67 W with a drain efficiency of 80%, PAE of 71% and a compressed gain of 9.3 dB. The entire array gives 2.24 W at 5 GHz, which means that the power-combining efficiency is 84%. This is illustrated in Fig. 12, which shows the power sweep of the single element with superimposed values for the array output power per element at 18 dBm input power. The measured frequency dependence of the output power, drain efficiency, and PAE is shown in Fig. 13.

## VI. ACKNOWLEDGMENT

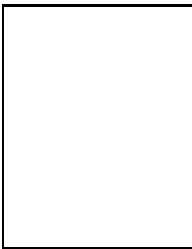
This work was funded by the Army Research Office, by Lockheed-Martin, and by the NSF Presidential Faculty Fellow Award. The authors would also like to thank Hughes for donating devices and Dr. Reza Tayrani of Compact Software for many helpful discussions, as well as for providing devices and a nonlinear Materka model.

## REFERENCES

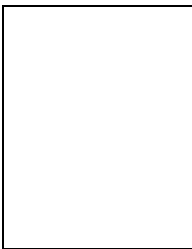
- [1] T. Shimura, M. Sakai, A. Inoue, S. Izumi, H. Matsuoka, J. Udomoto, K. Kosaki, T. Kuragaki, R. Hattori, H. Takano, T. Sonoda, S. Takamiya, and S. Mitsui, "1 W Ku-Band AlGaAs/GaAs

- power HBTs with 72% peak power-added efficiency," in *1994 IEEE MTT-S Int. Microwave Symp. Dig.*, San Diego, CA, pp. 687-690, May 1994.
- [2] M. Matlobian, A. Brown, L. Nguyen, M. Melendes, L. Larson, M. Delaney, M. Thompson, R. Rhodes, and J. Pence, "20-GHz high-efficiency AlInAs-GaInAs on InP power HEMT," *IEEE Microwave and Guided Wave Lett.*, vol. 3, no. 5, pp. 142-144, May 1993.
  - [3] J. Chi, J. Lester, Y. Hwang, P. Chow, and M. Huang, "A 1-W high-efficiency Q-Band MMIC power amplifier," *IEEE Microwave and Guided Wave Lett.*, vol. 5, no. 1, pp. 21-23, Jan. 1995.
  - [4] V.J. Tyler, "A new high efficiency high power amplifier," *Marconi Rev.*, vol. 21, pp. 96-109, 1958.
  - [5] D. Snider, "A theoretical analysis and experimental confirmation of the optimally loaded and overdriven RF power amplifier," *IEEE Trans. on Electron Devices*, vol. 14, no. 12, pp. 851-857, Dec. 1967.
  - [6] H. Krauss, C. Bostian, and F. Raab, *Solid-State Radio Engineering*. New York: John Wiley & Sons. 1980.
  - [7] C Duvanaud, S. Dietsche, G. Pataut, and J. Obregon, "High efficient class F GaAs FET amplifiers operating with very low bias voltages for use in mobile telephones at 1.75 GHz," *IEEE Microwave and Guided Wave Lett.*, vol. 3, no. 8, pp. 268-270, Aug. 1993.
  - [8] L. Hall and R. Trew, "Maximum efficiency tuning of microwave amplifiers," in *1991 IEEE MTT-S Int. Microwave Symp. Dig.*, Boston, MA, pp. 123-126, June 1991.
  - [9] M. Maeda, H. Takehara, M. Nakamura, Y. Ota and O. Ishikawa, "A high power and high efficiency amplifier with controlled second-harmonic source impedance," in *1995 IEEE MTT-S Int. Microwave Symp. Dig.*, Orlando, FL, pp. 579-582, May 1995.
  - [10] N.A. Sokal and A.D. Sokal, "Class-E - A new class of high-efficiency tuned single-ended switching power amplifiers," *IEEE Journal of Solid-State Circuits*, vol. SC-10, No. 3, pp. 168-176, June 1975.
  - [11] F.H. Raab, "Idealized operation of the class-E tuned power amplifier," *IEEE Trans. Circuits Syst.*, vol. CAS-24, no. 12, pp. 725-735, Dec. 1977.
  - [12] T.B. Mader and Z.B. Popović, "The transmission-line class-E amplifier," *IEEE Microwave and Guided Wave Lett.*, vol. 5, no. 9, pp. 290-292, Sept. 1995.
  - [13] T.B. Mader, *Quasi-Optical Class-E Power Amplifiers*, Ph.D. dissertation, Univ. of Colorado, Boulder, Aug. 1995.
  - [14] F.H. Raab, "Suboptimum operation of class-E power amplifiers," in *Proc. RF Technology Expo 89*, Santa Clara, CA, pp. 85-98 Feb. 1989.
  - [15] N. Sokal and R. Redl, "Power transistor output port model," *RF Design*, pp. 45-51, June 1987.
  - [16] *Microwave Harmonica PC Version 6.0*, Compact Software Inc., Paterson, New Jersey.
  - [17] A. Materka and T. Kacprzak, "Computer calculation of large signal GaAs FET amplifier characteristics," *IEEE Trans. Microwave Theory Tech.*, vol. MTT-33, no. 2, Feb. 1985.
  - [18] M. Kim, E. Sovero, J. Hacker, M. De Lisio, J. Chiao, S. Li, D. Gagnon, J. Rosenberg, and D. Rutledge, "A 100-element HBT grid amplifier," *IEEE Trans. Microwave Theory Tech.*, vol. MTT-41, no. 10, pp. 1762-1771, Oct. 1993.
  - [19] J. Schoenberg, T. Mader, B. Shaw, and Z.B. Popović, "Quasi-optical antenna array amplifiers," in *1995 IEEE MTT-S Int. Microwave Symp. Dig.*, Orlando, FL, pp. 605-608, May 1995.

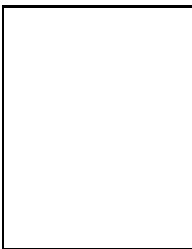
interests include nonlinear, high-efficiency microwave/mm-wave and photonic (fiber-based) power amplifiers, as well as high-speed digital techniques and communication systems.



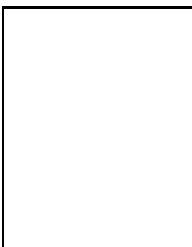
**Eric W. Bryerton** (S'95) was born in Chicago, IL on May 30, 1974. He received the BSEE from the University of Illinois, Urbana in 1995, the MSEE from the University of Colorado, Boulder in 1997, and is currently working toward the Ph.D. in electrical engineering. His research interests include microwave/mm-wave power amplifiers, free-space power combiners, and low-power resonant electro-optic modulators.



**Milica Marković** (S'94-M'98) was born in Belgrade, Serbia, Yugoslavia on January 8, 1966. She received the Dipl.Ing. degree from the University of Belgrade in 1991, the M.S. and Ph.D. in electrical engineering from the University of Colorado, Boulder in 1994 and 1997 respectively. She is currently a Research Assistant Professor at Clarkson University. Her research interests include high-efficiency amplifiers, quasi-optical modulators, and free-space power combining.

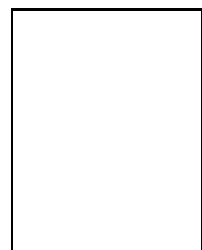


**Michael Forman** (S'95) received the BSEE and MSEE from the University of Colorado, Boulder in 1996 and 1998 respectively, and is currently working towards the Ph.D. in electrical engineering. His research interests include microwave and millimeter-wave planar amplifiers and phase locked loops.



**Zoya Popović** (S'86-M'90) received her Dipl.Ing. degree from the University of Belgrade, Serbia, Yugoslavia, in 1985, and her Ph.D. degree from Caltech, Pasadena in 1990. She is currently an Associate Professor of electrical engineering at the University of Colorado at Boulder. Her research interests include microwave and millimeter-wave quasi-optical techniques, microwave and millimeter-wave active antennas and circuits, and RF photonics. Dr. Popović received the IEEE Microwave

Theory and Techniques Microwave Prize, the URSI Young Scientist Award, and the National Science Foundation Presidential Faculty Fellow Award in 1993. She was awarded the International URSI Isaac Koga Gold Medal in 1996.



**Thomas B. Mader** (S'90-M'96) was born in San Francisco, CA on December 11, 1967. He received the BSEE from U.C. Berkeley in 1990 and a Ph.D. in electrical engineering from the University of Colorado, Boulder in 1995. Early work experience was with Siemens GMBH in Switzerland, as well as Tandem Computers and Apple Computer in Cupertino, CA. At Apple he received his first patent on a digital termination circuit. Currently he is working at Hughes Space and Communications in Los Angeles, CA, where his work spans microwave through optical frequency ranges, and he currently has two more patents pending. His research